Synthesis of Copper Chloride and Cobalt Chloride Doped Polyanilines and Their Magnetic and Alternating-Current Transport Properties

K. Gupta,[1] G. Chakraborty,[1] S. Ghatak,[1] P. C. Jana,[2] A. K. Meikap[1]

[1]National Institute of Technology, Mahatma Gandhi Avenue, Durgapur 713209, West Bengal, India
[2]Department of Physics and Technophysics, Vidyasagar University, Midnapore 721102, West Bengal, India

ABSTRACT: Polyaniline (PANI) was synthesized by the well-known oxidative polymerization of aniline with ammonium peroxodisulfate as the oxidant. The morphological, structural, thermal, optical, magnetic, and electrical properties were characterized with scanning electron microscopy, X-ray diffraction, Fourier transform infrared, thermogravimetric analysis, differential scanning calorimetry, ultraviolet–visible spectroscopy, room-temperature magnetic measurements, and low-temperature electrical transport measurements by the standard four-probe method. Greater thermal stability and crystallinity were observed in doped PANI versus pure PANI. Magnetic measurements showed that the magnetic susceptibility was field-dependent. Positive and negative susceptibility values were observed. This may have been due to the interactions of magnetic ions among interchains or intrachains of the polymer matrix. The alternating-current (ac) conductivity was measured in the temperature range of 77–300 K in the frequency range of 20 Hz to 1 MHz. The frequency-dependent real part of the complex ac conductivity was found to follow the universal dielectric response: $\sigma'(f) \propto f^s$ [where $\sigma'(f)$ is the frequency-dependent total conductivity, f is the frequency, and s is the frequency exponent] The trend in the variation of the frequency exponent with temperature corroborated the fact that correlated barrier hopping was the dominant charge-transport mechanism for PANI–CoCl$_2$. An anomalous dependence on temperature of the frequency exponent was observed for PANI–CuCl$_2$. This anomalous behavior could not be explained in terms of existing theories. © 2009 Wiley Periodicals, Inc. J Appl Polym Sci 115: 2911–2917, 2010

Key words: charge transport; conducting polymers; FT-IR; metal-polymer complexes; thermogravimetric analysis (TGA)

INTRODUCTION

Polymers are generally amorphous insulator materials. However, during the last $2\frac{1}{2}$ decades, a new class of organic polymers has been synthesized with the ability to conduct electric current. These polymers are known as conducting polymers. The common feature of most electrically conducting polymers is the presence of an extended π-conjugation system with single- and double-bond alteration along the polymer backbone. Conducting polymers are semiconductor materials with low charge carrier mobility.[1–15] The conductivity of this type of polymer can be enhanced up to the metallic range by doping.[16,17] Beside the electrical properties, the unique magnetic, optical, and chemical properties of conducting polymers have led to a wide range of technological applications in electromagnetic interference shielding, rechargeable batteries, electrodes, sensors, corrosion protection coatings, and microwave absorption.[18–27] The beauty of this class of materials is that the properties can be tuned by doping. Among the different conducting polymers, polyaniline (PANI) has attracted much attention in recent years because it can be synthesized easily, is comparatively stable in air, is relatively cheap, is soluble in various solvents, and exhibits a number of properties, such as optical, electrical, and magnetic properties.[28,29] The conductivity of these heterogeneous systems depends on a number of factors, such as the concentration of the conducting fillers, their shape, size, and orientation, and the interfacial interaction between the filler molecules and host matrix; the conductivity also depends on the reaction temperature, time of polymerization, monomer-to-oxidant molar ratio, and oxidizing agent. The geometrical shape of the dispersant governs the capacity for conductive network formation, which results in a large increase in the conductivity.[30] Dopant selection plays a significant role because the dopant can control

different properties of the polymers. A dopant can cause structural disorder in the polymer chains, and as a result, charge defects can occur in the polymer matrix. Selection of the optimum parameters for synthesis can reduce the disorder and help to promote the conductivity of the polymers.[31–36] Generally, the carriers in the process of doping in conducting polymers are known to be self-trapped by the conjugated polymeric chains in the form of polarons and bipolarons.[37] Our motivation for this investigation was to study, from low temperatures to high temperatures (77–300 K), the effects of the magnetic properties of PANI doped with some magnetic ions and also to study the tailoring of the electrical and magnetic properties of PANI.

In this study, we synthesized PANIs doped with different dopants [copper chloride ($CuCl_2$) and cobalt chloride ($CoCl_2$)] and characterized them with scanning electron microscopy (SEM), X-ray diffraction (XRD), Fourier transform infrared (FTIR), thermogravimetric analysis (TGA), differential scanning calorimetry (DSC), and ultraviolet–visible (UV–vis) spectroscopy. The ac conductivity of the samples was measured in the temperature range of 77–300 K and in the frequency range of 20 Hz to 1 MHz, and the room-temperature magnetic susceptibility of the samples was also measured.

EXPERIMENTAL

Materials

Aniline, $CuCl_2$, $CoCl_2$, hydrochloric acid (HCl), ammonium peroxodisulfate, acetone, and ethanol were used as received from the market and were purified as required for the investigation.

Synthesis of PANI

Aniline was double-distilled *in vacuo*. Solutions ($0.01M$) of different dopants were prepared. Twenty milliliters of $0.01M$ aniline was mixed with 20 mL of a $0.01M$ dopant solution with continuous magnetic stirring. A homogeneous solution was obtained. A $0.5M$ ammonium peroxodisulfate solution was prepared in 10 mL of $1M$ HCl and kept at 0°C for 30 min. It was then added dropwise with continuous magnetic stirring, and the solution was left at rest to polymerize for 24 h at 0°C. The samples were collected on a filter and washed with acetone, ethanol, and water to remove the monomer, oligomer, and excess oxidant. The samples were dried in an oven at 40°C overnight. Samples marked as A, B, and C were PANI, $CuCl_2$-doped PANI, and $CoCl_2$-doped PANI, respectively.

Characterization

The morphology of these samples was measured with a Hitachi (Tokyo, Japan) S-3000N scanning electron microscope on a gold substrate. The phase identification of the finely powdered composites and polymer was performed with an X'Pert Pro X-ray diffractometer with nickel-filtered Cu Kα radiation (wavelength = 1.5414 Å) in the 2θ range of 20–80°. TGA of the samples was carried out on a PerkinElmer Pyris 1 TGA instrument at a heating rate of 10°C/min under an N_2 atmosphere over a temperature range of 20 to 900°C. DSC analysis was carried out with a PerkinElmer Pyris Diamond differential scanning calorimeter. FTIR spectra were recorded with a Nicolet Nexus FTIR instrument in the region of 500–4000 cm^{-1} with KBr pellets. The UV–vis spectra of the samples were taken with a U-3010 double-beam spectrophotometer (Waltham, MA) with dimethyl sulfoxide as the solvent. Magnetic susceptibility measurements were performed by Gouy's method at room temperature. The low-temperature alternating-current (ac) conductivity was measured by the standard four-probe method in the temperature range of 77–300 K and in the frequency range of 20 Hz to 1 MHz.

RESULTS AND DISCUSSION

Morphology

Figure 1(a,b) shows the morphology of the $CuCl_2$- and $CoCl_2$-doped PANIs. From the SEM images, we can observe that the grains were well resolved and circular, and from the energy-dispersive spectroscopy analysis of different portions of the SEM images, we can also confirm that dopant particles were uniformly distributed in the polymer matrix. The uniform morphology was due to no polymer chain entanglement during the polymerization process.[38]

Structural characterization

XRD patterns of undoped PANI and doped PANI are presented in Figure 2. From the XRD patterns, we can observe that undoped PANI was amorphous, but $CuCl_2$- and $CoCl_2$-doped PANIs were crystalline. $CuCl_2$- and $CoCl_2$-doped PANIs showed monoclinic and hexagonal rhombohedral crystalline structures, respectively (Joint Committee on Powder Diffraction Standards nos. 01-0185 and 03-0869, respectively). The characteristic peaks were observed at 2θ values of 26.03, 30.80, 38.10, 50.67, 54.06, and 64.6 for $CuCl_2$-doped PANI and at 2θ values of 35.3, 51.19, and 63.72 for $CoCl_2$-doped PANI. This XRD study confirmed that $CuCl_2$ and $CoCl_2$ had been doped in the PANI matrix.
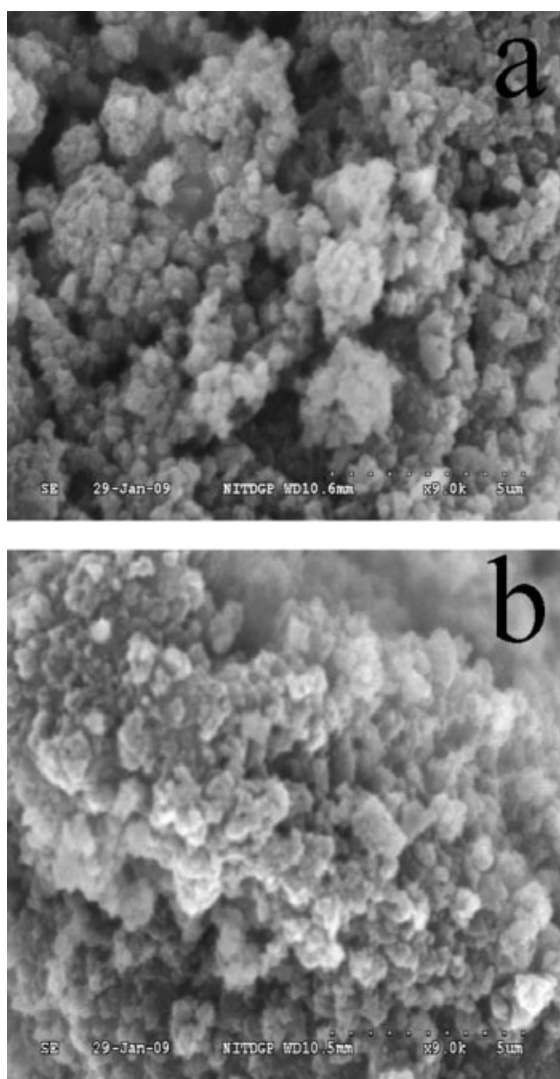
Figure 1 SEM images of (a) $CuCl_2$- and (b) $CuCl_2$-doped PANI.

FTIR spectra of doped and undoped PANIs are presented in Figure 3. Undoped PANI showed characteristic peaks at 1583.74, 1488.89, 1300.0, 1130, 818.74, and 681.92 cm^{-1}. The bands at 1583.74 and 1488.89 cm^{-1} were attributed to C=C and C=N stretching modes of vibration for the quinoid (—N=Q=N—, where Q is a quinoid ring) and benzoid units, whereas the band at 1300.0 cm^{-1} was assigned to the C—N stretching mode of the benzoid unit. The band at 1130 cm^{-1} was due to the quinoid unit of PANI. The band at 810 cm^{-1} was attributed to C—C and C—H stretching of the benzoid unit of PANI, and the band at 681.92 cm^{-1} was assigned to the out-of-plane C—H vibration. The peak assignment revealed that the produced product was PANI. The incorporation of $CuCl_2$ and $CoCl_2$ into the PANI matrix led to small shifts of the peaks and also decreases in the intensities of the peaks; this indicated structural changes in the polymer that

occurred with doping. The bands at 1583.74, 1488.89, and 1300.0 cm^{-1} were shifted in doped PANI, and this indicated the molecular interactions of the dopants with different reaction sites of PANI. This FTIR spectrum analysis also confirmed that $CuCl_2$ and $CoCl_2$ had been doped in the PANI matrix.[39]

Thermal stability

TGA of doped PANI and undoped PANI is presented in Figure 4. The thermogram of undoped PANI shows that the mass loss began around 50°C and continued up to 100°C. The mass loss remained steady up to 350°C, and then rapid mass loss occurred up to 625°C. The initial mass loss was due to the loss of water molecules, and after that, rapid mass loss occurred because of the degradation of the polymer chain. However, in doped PANI, the mass loss remained constant up to 420°C, and then mass loss occurred slowly up to 530°C because of the removal of dopant molecules from the polymer structure.[40] Rapid mass loss occurred after 530°C because of the rapid degradation of the polymer chains.[41] TGA indicated better thermal stability of the doped PANI versus the undoped PANI, and $CoCl_2$-doped PANI was more stable than $CuCl_2$-doped PANI. The better thermal stability of doped PANI could be explained by the dominance of the benzenoid structure. Alternatively, the inferior thermal stability of pure undoped PANI was due to the presence of a quinoid ring in its structure.

Figure 5 shows DSC thermograms of doped PANI and undoped PANI. The glass-transition temperature increased from pure undoped PANI to doped PANI (from 125 to 145°C), and change of enthalpy
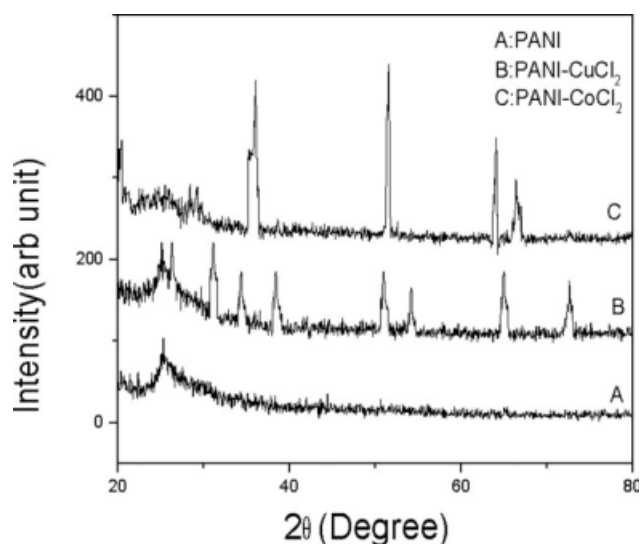

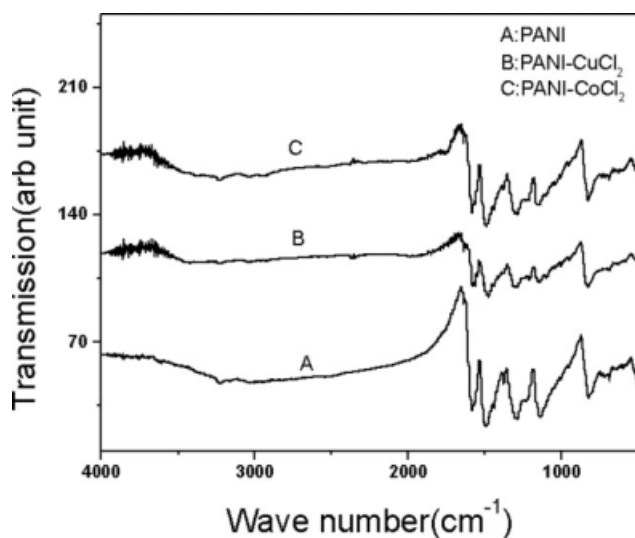**Figure 2** XRD of PANI and $CuCl_2$- and $CuCl_2$-doped PANI.

Figure 3 TGA of PANI and CuCl$_2$- and CuCl$_2$-doped PANI.

Figure 5 DSC of PANI and CuCl$_2$- and CuCl$_2$-doped PANI.

(ΔH) also increased with doping; this indicated the greater thermal stability and crystallinity of doped PANI. It was also observed that CoCl$_2$-doped PANI was more stable than CuCl$_2$-doped PANI. These results also support the TGA observation that doped PANI was thermally more stable than undoped PANI.

Optical characterization

UV–vis absorption spectra of PANI and doped PANI are presented in Figure 6. Undoped PANI mainly showed two absorption bands at 293–300 and 558–620 nm. The first one was attributed to the π–π* transition in the benzoid rings, and the second one was due to exciton absorption of the quinoid rings.[41,42] However, for doped PANI, a blueshift of
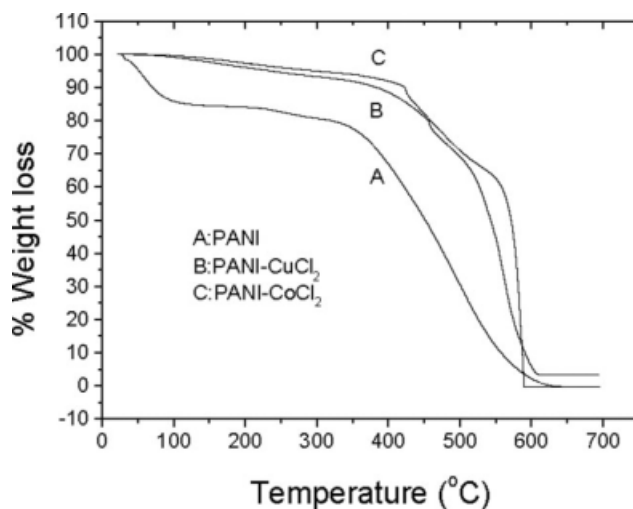
the absorption bands occurred. The absorption band due to the π–π* transition in the benzoid rings shifted to 270 nm for CoCl$_2$-doped PANI and to 288 nm for CuCl$_2$-doped PANI. The exciton absorption band of the quinoid rings shifted to a lower wavelength with a much lower intensity. This also supported the dominance of the benzoid ring as evidenced by TGA. The shape of the curve depended on the carrier concentration, lifetime, and transition energy. The broad and narrow peaks were contributions of delocalized and localized charge carriers. The electrical conductivity depended on the mobility of these charge carriers. The electrical conductivity of doped PANI increased, and this may have been due to the increase in the mobility of these charge carriers.
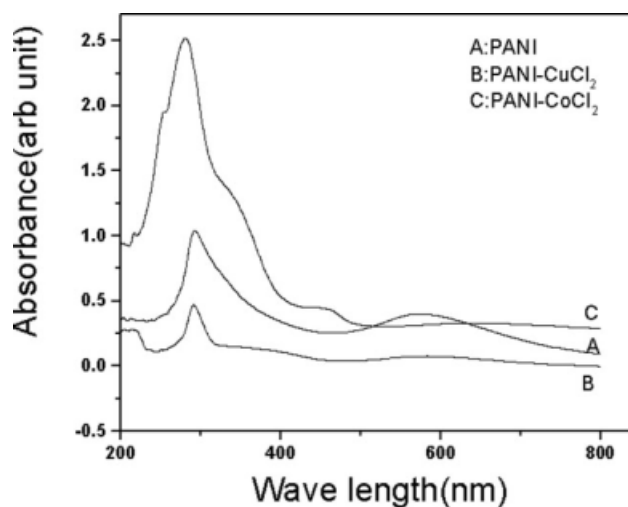

Figure 4 FTIR of PANI and CuCl$_2$- and CuCl$_2$-doped PANI.

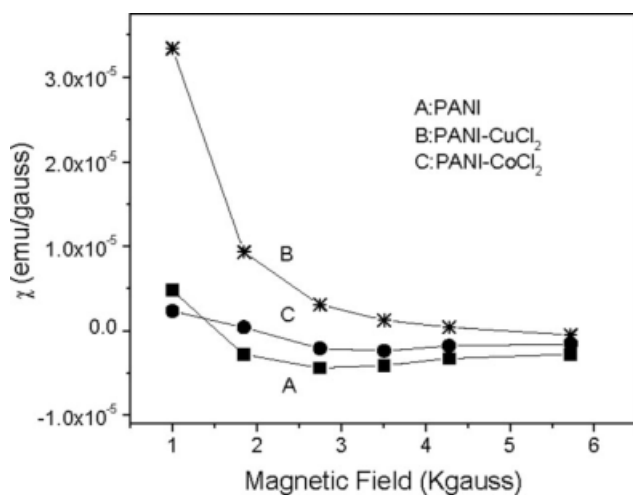**Figure 6** UV–vis spectra of PANI and CuCl$_2$- and CuCl$_2$-doped PANI.

Figure 7 Plot of the magnetic susceptibility (χ) versus the magnetic field for PANI and CuCl$_2$- and CuCl$_2$-doped PANI.

Magnetic property study

Magnetic susceptibility values of doped PANI and undoped PANI are presented in Figure 7. The magnetic susceptibility was measured from 1 to 5 kG. The magnetic susceptibility of doped PANI was enhanced in comparison with undoped PANI. It was also observed that the magnetic susceptibility varied with the field. In the case of CuCl$_2$-doped PANI, the magnetic susceptibility decreased with an increase in the field, but its value remained positive throughout. For CoCl$_2$-doped PANI, the magnetic susceptibility decreased with an increase in the field, but its value became negative as the field increased. The susceptibility of these materials could be explained by the assumption of interactions between the magnetic ions linked with the polymer chain via exchange interactions. To explain, we used a simple formula:

$$\chi = \chi_{pauli}/(1 - \lambda_{exchange})$$

where χ is the susceptibility for interacting conduction electrons;[43] χ_{pauli} is the Pauli susceptibility for noninteracting conduction electrons; and $\lambda_{exchange}$ is the exchange wavelength, which depends on the density of interacting electrons (N), the interaction energy (U), and the Fermi energy (E_f; $\lambda_{exchange} = 3NU/4E_f$). When $\lambda_{exchange}$ is greater than 1, χ becomes negative; it has been assumed to be different for different samples. Depending on the doping concentration, a dopant–polymer interaction takes place, and in high fields, the energy levels of dopants are such that $3NU > 4E_f$. Therefore, in a high field, χ becomes negative. It was observed from the magnetic susceptibility data that CuCl$_2$-doped PANI

behaved as a better magnetic material than CoCl$_2$-doped PANI in a low field, and in a high field, both doped and undoped samples showed almost the same magnetic behavior.

Study of the ac conductivity

The ac conductivity of PANI with different dopants was investigated in the frequency range of 20 Hz to 1 MHz and in the temperature range of 77–300 K. The measured data showed that the variation of the conductivity with the frequency at a particular temperature was prominent at higher frequencies, whereas at low frequencies, it was almost independent of the frequency; this could be attributed to the direct-current contribution. A general feature of amorphous semiconductors or disordered systems is that the frequency-dependent alternating-current conductivity [$\sigma_{ac}(f)$] obeys a power law with the frequency. The frequency-dependent total conductivity [$\sigma'(f)$] at a particular temperature over a wide range of frequencies can be expressed as follows[44–46]:

$$\sigma'(f) = \sigma_{dc} + \sigma_{ac}(f) = \sigma_{dc} + \alpha f^s \tag{1}$$

where σ_{dc} is the direct-current conductivity, α is the temperature-dependent constant, f is the frequency, and s is the frequency exponent (<1). The value of $\sigma_{ac}(f)$ was determined upon subtraction of the direct-current contribution from $\sigma'(f)$. Figure 8 shows the linear variation of $\ln \sigma_{ac}(f)$ with $\ln f$ at different temperatures for the PANI–CoCl$_2$ sample. Similar behavior was observed for all other samples. The value of s at each temperature was calculated from the slope of the $\ln \sigma_{ac}(f)$–$\ln f$ plot for each temperature. The trend of the changes in s with temperature
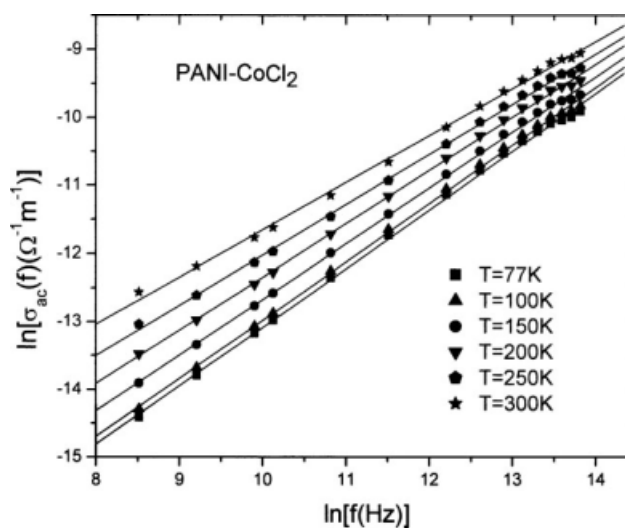

Figure 8 Frequency (f) dependence of the alternating-current conductivity [$\sigma_{ac}(f)$] at different temperatures for PANI–CoCl$_2$.
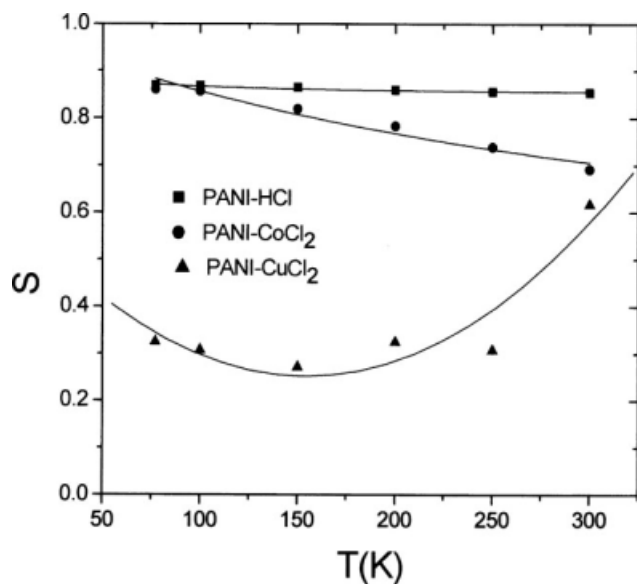
Figure 9 Frequency exponent (s) versus the temperature (T) for different samples.

is shown in Figure 9 for different samples. s was found to be weakly temperature-dependent for the PANI samples. For the PANI–CoCl$_2$ sample, the estimated values of s gradually decreased with increasing temperature, but for the PANI–CuCl$_2$ sample, it first decreased and then increased. In general, two physical processes, such as correlated barrier hopping (CBH)[46] and quantum mechanical tunneling (electron tunneling,[47] small polaron tunneling,[46] and large polaron tunneling[45]), govern the conduction process of disordered systems. As the nature of the temperature dependence of s is different for different conduction processes, the exact nature of charge transport can be obtained experimentally from the temperature variation of s. According to the electron tunneling theory, s is temperature-independent, whereas for small polaron tunneling, s increases with increasing temperature, and for large polaron tunneling, s decreases first and then increases with increasing temperature. However, according to the CBH model, s decreases only with an increase in temperature. From the trend of changes in s with temperature for the PANI–CoCl$_2$ sample, it is presumed that the CBH model is suitable for explaining the behavior of our data. According to this model, the charge carrier hops between the sites over the potential barrier separating them, and s is given by the following expression[46]:

$$s = 1 - \frac{6k_BT}{W_H - k_BT \ln\left(\frac{1}{\omega\tau_0}\right)} \quad (2)$$

where W_H is the effective barrier height, k_B is the Boltzmann constant, T is the temperature, $\omega(=2\pi f)$ is

the angular frequency, and τ_0 is the characteristic relaxation time. According to eq. (2), for large values of W_H/k_BT, the variation of s with frequency is so small that it is effectively independent of the frequency.[48] Moreover, it was observed in our study that s was independent of the frequency [linear variation of ln $\sigma_{ac}(f)$ with ln f in Fig. 8]. Therefore, we fitted our experimental data with eq. (2) as a function of temperature alone with W_H and $\omega\tau_0$ as fitting parameters. In Figure 9, the points represent the experimental data, whereas the solid lines are the theoretical best fit values obtained from eq. (2) for the PANI–CoCl$_2$ sample. The best fitted values of parameters W_H and τ_0 (at a fixed frequency of 1 MHz) were 0.28 eV and 2.73 × 10^{-3} s, respectively. However, for the PANI sample, the value of s decreased slowly and followed a linear variation, as shown in Figure 9. According to the theory of the CBH model, at lower temperatures at which the value of W_H/k_BT is large, eq. (2) transforms into a linear temperature dependence of s. Therefore, the observed linear temperature dependence of s may be due to the high value of W_H/k_BT at low temperatures, and the value of W_H obtained from this linear fit was 1.16 eV. Therefore, from the trend of the variation of s with temperature, it can be concluded that the ac conductivity in the investigated samples (PANI and PANI–CoCl$_2$) can be described by the CBH model. From the nature of the variation of s with temperature for the PANI–CuCl$_2$ sample, we presume that the large polaron tunneling model may be suitable for analyzing the temperature dependence of s. We tried to fit the experimental data to this theory, but the theory did not match the data, and the fit yielded nonphysical values of the parameters. Therefore, the anomalous behavior of s for the PANI–CuCl$_2$ sample cannot be understood in terms of existing theories. Hence, more studies are necessary to formulate the true mechanism in this system.

CONCLUSIONS

In summary, we synthesized CuCl$_2$- and CoCl$_2$-doped PANIs by the chemical oxidation method. Doped PANI was more thermally stable and more crystalline than undoped PANI. Confirmation of the doping of PANI by CuCl$_2$ and CoCl$_2$ was obtained by XRD and FTIR analysis. Unusual magnetic-field-dependent susceptibility was obtained. In high magnetic fields, the energy levels of the dopants were such that χ became negative, and in low magnetic fields, the energy levels of the dopants were such that χ became positive. In low magnetic fields, CuCl$_2$-doped PANI is a promising magnetic sensor material. The frequency-dependent real part of the complex ac conductivity was found to follow the

universal dielectric response: $\sigma'(f) \propto f^s$. The trend in the variation of s with temperature corroborated the fact that CBH was the dominant charge-transport mechanism for the PANI and PANI–CoCl$_2$ samples. We observed an anomalous dependence on temperature of s for the PANI–CuCl$_2$ sample. This anomalous behavior cannot be explained in terms of existing theories. Therefore, electrical transport and magnetic properties of PANI can easily be tailored by the doping of PANI with a suitable dopant.

References

1. Heeger, A. J. Rev Mod Phys 2001, 73, 681.
2. Menon, R.; Yoon, C. O.; Moses, D.; Heeger, A. J. In Handbook of Conducting Polymers, 2nd ed.; Skotheim, T. A.; Elsenbaumer, R. L.; Reynolds, J. R., Eds.; Marcel Dekker: New York, 1998.
3. Heeger, A. J. Phys Scr 2002, T102, 30.
4. Kaiser, A. B. Adv Mater 2001, 13, 927.
5. Kiebooms, R.; Menon, R.; Lee, K. In Handbook of Advanced Electronic and Photonic Materials and Devices; Nalwa, H. S., Ed.; Academic: San Diego, 2001; Vol. 8.
6. Kohlman, R. S.; Joo, J.; Epstein, A. J. In Physical Properties of Polymers Handbook; Mark, J. E., Ed.; AIP: New York, 1996.
7. Lee, K. In Encyclopedia of Nanoscience and Nanotechnology; Nalwa, H. S., Ed.; American Scientific: San Diego, 2004; Vol. 5.
8. Lee, S. H.; Lee, D. H.; Lee, K.; Lee, C.-W. Adv Funct Mater 2005, 15, 1495.
9. Ashcroft, N. W.; Mermin, N. D. Solid State Physics; Saunders College: New York, 1976.
10. Landau, L. D. Sov Phys JETP 1957, 3, 920.
11. Pines, I. D.; Nozieres, P. The Theory of Quantum Liquids; Benjamin: Menlo Park, CA, 1966.
12. Mott, N. F. Metal–Insulator Transitions; Taylor & Francis: London, 1990.
13. Anderson, P. W. Solid State Phys 1970, 2, 193.
14. Fite, C.; Cao, Y.; Heeger, A. J. Solid State Commun 1990, 73, 607.
15. Park, Y. W.; Choi, E. S.; Suh, D. S. Synth Met 1998, 96, 81.
16. Lee, K.; Chio, S.; Park, S. H.; Heeger, A. J.; Loo, C.; Lee; S. H. Nat Lett 2006, 441, 65.
17. Chaudhuri, D.; Kumar, A.; Rudra, I.; Sharma, D. D. Adv Mater 2001, 13, 1548.
18. Aphesteguy, J. C.; Bercoff, P. G.; Jacobo, S. E. Phys B 2007, 398, 200.
19. Bartlett, P. N.; Birkin, P. R. Synth Met 1993, 61, 15.
20. Naarman, H. Science and Application of Conducting Polymers; Adam Hilger: Bristol, England, 1991.
21. Joo, J.; Epstein, A. J Appl Phys Lett 1994, 65, 2278.
22. Bartlett, P. N.; Birkin, P. R. Synth Met 1993, 61, 15.
23. Osaheni, J. A.; Jenekhe, A. S.; Vanherzeele, H.; Meth, J. S.; Sun, Y.; MacDiarmid, A. G. J Phys Chem 1992, 96, 2830.
24. Kobayashi, T.; Yoneyama, H.; Tamura, H. J Electroanal Chem 1984, 161, 419.
25. Hau, Z.; Shi, J.; Zhang, L.; Ruan, M.; Yan, J. Adv Mater 2002, 14, 830.
26. Levi, B. G. Phys Today 2000, 53, 19.
27. Asim, N.; Radiman, S.; Bin Yarmo, M. A. Mater Lett 2008, 62, 1044.
28. Gupta, C. M.; Umare, S. S. Macromolecules 1992, 25, 138.
29. Mizzoguchi, K. Synth Met 2001, 119, 35.
30. Pant, H. C.; Patra, M. K.; Negi, S. C.; Bhatia, A.; Vadera, S. R.; Kumar, N. Bull Mater Sci 2006, 29, 379.
31. Ghosh, P.; Sarkar, A.; Meikap, A. K.; Chattopadhyay, S. K.; Chatterjee, S. K.; Ghosh, M. J Phys D: Appl Phys 2006, 39, 3047.
32. Chiang, J. C.; MacDiarmid, A. G. Synth Met 1986, 13, 193.
33. Epstein, A. J.; MacDiarmid, A. G. Synth Met 1989, 18, 303.
34. Suubramanian, C. K.; Kaiser, A. B.; Gilberd, P. W.; Wessling, B. J Polym Sci Part B: Polym Phys 1993, 31, 1425.
35. Chakraborty, G.; Sarkar, A.; Ghosh, P; Meikap, A. K.; Chowdhury, P. Polym Eng Sci 2009, 49, 910.
36. Suzhu, Y.; Hing, P.; Xiao, H. J Appl Phys 2000, 88, 398.
37. Sanjai, B.; Raghunathan, A.; Natarajan, T. S.; Rangarajan, G. Phys Rev B 1997, 55, 10734.
38. Reddy, K.; Lee, K. P.; Lee, Y.; Gopalan, A. I. Mater Lett 2008, 62, 1815.
39. Dey, A.; De, S.; De, A.; De, S. K. Nanotechnology 2004, 15, 1277.
40. Palaniappan, S.; Narayana, B. H. J Polym Sci Part A: Polym Chem 1994, 32, 2431.
41. Erdem, E.; Karakisla, M.; Sacak, M. Eur Polym J 2004, 40, 785.
42. Ding, S.; Mao, H.; Zhang, W. J Appl Polym Sci 2008, 109, 2842.
43. Kahol, P. K. Solid State Commun 2002, 124, 93.
44. Mott, N. F.; Davis, E. A. Electronic Processes in Non-Crystalline Materials, 2nd ed.; Oxford: Clarendon, England, 1979.
45. Long, A. R. Adv Phys 1982, 31, 553.
46. Elliott, S. R. Adv Phys 1987, 36, 135.
47. Efros, A. L. Philos Mag B 1981, 43, 829.
48. Ghosh, M.; Barman, A.; De, S. K.; Chatterjee, S. J Appl Phys 1998, 84, 806.